www.dergipark.gov.tr
ISSN:2148-3736

El-Cezerî Fen ve Mühendislik Dergisi
Cilt: 9, No: 3, 2022 (1122-1135)

El-Cezerî Journal of Science and Engineering
Vol: 9, No: 3, 2022 (1122-1135)
DOI : 10.31202/ecjse.1123584

ECJSE

Research Paper / Makale

Investigation of Structural and Magnetic Properties of Co, Ni and CoNi Alloy Thin Films by Fabricated with Electrodeposition

Rasim ÖZDEMİR[1a], Cuma Ali KORKMAZ[2b]

[1]Kilis 7 Aralık University, Department of Electricity and Energy, Kilis, Turkiye
[2]Kilis 7 Aralık University, Department of Physics, Kilis, Turkiye
rozdemir@kilis.edu.tr

Received/Geliş: 31.05.2022 **Accepted/Kabul:** 27.08.2022

Abstract: The production of nanoparticles as thin film coating performed with electrodeposition method is easier and cheaper than other methods. Because, thin film production can be controlled with the change of ingredients in the bath composition. In this study, cobalt (Co), nickel (Ni), and cobalt-nickel (CoNi) alloy thin films were fabricated with electrodeposition method through the bath composition that consists of cobalt sulphate ($CoSO_4.7H_2O$), nickel sulphate ($NiSO_4.6H_2O$), nickel (II) chloride ($NiCl_2$ $6H_2O$) and boric acid (H_3BO_3). Crystal structure (XRD), morphological (SEM), elemental composition (ICP) and magnetic properties (VSM) of the fabricated thin films were investigated. Chemical properties of coating bath (CV) were examined as well. Magnetization measurements of the thin films were performed by applying magnetic fields between + 75000 Oe and -75000 Oe and then hysteresis loops were obtained. The Co, Ni, and CoNi films showed ferromagnetic material properties. Coercivity (Hc), permanent magnetization (Mr), saturation magnetization (Ms) values of these alloys were significantly affected by the amount of the Co, magneto crystal anisotropy and grain size. It was understood that some materials having hard and soft magnetic properties can be fabricated by controlling the bath composition.

Keywords: Electrodeposition, hydrogen evolution, cobalt-nickel alloy, magnetization, thin films

Elektrodepolama ile Üretilen Co, Ni ve CoNi Alaşımlı İnce Filmlerin Yapısal ve Manyetik Özelliklerinin İncelenmesi

Öz: Elektrodepolama yöntemi ile nano parçacıkların ince film kaplama olarak üretimi diğer yöntemlere göre daha kolay ve ucuz yapılmaktadır. Bunun nedeni, ince film üretiminin banyo içeriğindeki bileşenlerin ve üretim şartlarının değişimi ile kontrol edilebilmesidir. Bu çalışmada, elektrodepolama yöntemiyle, kobalt sülfat ($CoSO_4.7H_2O$), nikel sülfat ($NiSO_4.6H_2O$), nikel (II) klorür ($NiCl_2.6H_2O$) ve borik asit (H_3BO_3) den oluşan banyo kompozisyonundan saf kobalt (Co), nikel (Ni) ve kobalt-nikel (CoNi) alaşımlı ince filmler üretildi. Üretilen ince filmlerin kristal yapısı (XRD), morfolojisi (SEM), element bileşimi (ICP) ve manyetik özellikleri (VSM) incelendi. Kaplama banyosunun kimyasal özellikleri de dönüşümlü voltametri (CV) yöntemiyle incelendi. İnce filmlerin manyetizasyon ölçümleri + 75000 Oe ile -75000 Oe arasında manyetik alan uygulanarak yapıldı ve histerezis döngüleri elde edildi. Üretilen Co, Ni ve CoNi filmleri ferromanyetik malzeme özellikleri gösterdi. Bu alaşımların koversite (Hc), kalıcı mıknatıslanma (Mr) ve doyum mıknatıslanma (Ms) değerleri; Co miktarı, manyeto kristal anizotropi ve tane boyutundan önemli ölçüde etkilendi. Yapılan çalışmada, banyo bileşimi kontrol edilerek sert ve yumuşak manyetik özelliklere sahip malzemelerin üretilebileceği anlaşıldı.

Anahtar Kelimeler: elektrodepozisyon, histerezis döngüsü, kobalt-nikel alaşımı, manyetizasyon, ince filmler

How to cite this article
Özdemir, R., Korkmaz, C.A., "Investigation of Structural and Magnetic Properties of Co, Ni and CoNi Alloy Thin Films by Fabricated with Electrodeposition", El-Cezerî Journal of Science and Engineering, 2022, 9 (3); 1122-1135.

Bu makaleye atıf yapmak için
Özdemir, R, Korkmaz, CA., "Elektrodepolama ile Üretilen Co, Ni ve CoNi Alaşımlı İnce Filmlerin Yapısal ve Manyetik Özelliklerinin İncelenmesi", El-Cezerî Fen ve Mühendislik Dergisi, 2022, 9 (3); 1122-1135.
ORCID: [a] 0000-0003-1439-0444; [b]0000-0002-3546-7482

1. Introduction

Cobalt-nickel (CoNi) alloys are high quality engineering materials having high strength, good wear resistance, corrosion resistance, hardness, nuclear power systems, thermal conductivity, electrocatalytic and magnetic properties [1-4]. It is known that CoNi alloys have excellent magnetic properties and also, they are superior to pure metals [5]. Especially in recent years, in industrial implementations, they are used in magnetic recording devices and microelectronic devices, in addition, they are used for decorative purposes [6-7].

CoNi alloys can be fabricated by casting or coating methods. Thin film coatings are fabricated by methods such as electrochemical deposition (electrodeposition) [8-10], sol-gel [11-12], chemical vapor deposition [13], spray pyrolysis [14], physical vapor deposition [15], spin coating [16], dip coating [17], sputtering [18], electroless coating [19-20]. The electrodeposition system is one of the most popular methods for the production of magnetic films and alloys. It also has many advantages in the production of nanoparticles that are thin film coatings. In this method, the thin film coating process is much more favorable than the others due to some reasons: 1) production simplicity, 2) variety of deposition materials, 3) low-temperature processing and 4) control of the bath composition. In the electrodeposition process, the electrocatalytic property of the solution and the amount of energy consumed varies depending on the production conditions and the materials in the bath composition [21-23]. Fabrication of thin films by electrodeposition method is influenced by such factors as solution concentration, pH value, current density, additives, deposition (cathode) potentials, solution temperature, mixing of solution, continuous or pulsed current of the deposition [24-26].

Iron (Fe), Cobalt (Co), nickel (Ni) metals, and the compounds consisting of those such as CoNi, CoFe, and NiFe alloys are the most important ferromagnetic materials [27]. According to the coercivity (Hc) size, the ferromagnetic materials are grouped as hard magnetic or soft magnetic materials. If the Hc value of magnetic materials is less than 12.6 Oe, it is classified as soft magnetic material, if not, then hard magnetic material [28]. According to the Hc size, the ferromagnetic materials are grouped as hard magnetic or soft magnetic materials [29].

Soft magnetic materials with low Hc and having high saturation magnetization (Ms) are desired to develop devices such as magnetic read-write heads, relays, transformers, electromagnets and electric motors [29]. On the other hand, for electrical machines that require power generation and permanent magnetization (Mr), materials with hard magnetic properties are desired. Depending on the implementations, both hard and soft magnetic materials show different characteristics [30-31].

It is possible to produce various CoNi alloys by electrodeposition technique by changing the Co^{2+} and Ni^{2+} metal ion concentrations in the solution used in thin film production. The magnetic properties of produced alloys such as Hc, Mr, and Ms value vary greatly depending on the Co and Ni concentration in the deposited film content [32].

In recent years, especially in the electrodeposition of CoNi alloy materials; studies which focus on producing thin films with the smaller grain size, the smaller Hc, with soft magnetic properties material, by changing deposition conditions and additives in the bath have been researched. In this study, Co, Ni, and CoNi alloy thin films were fabricated by electrodeposition. And the deposition potential of thin films, concentration ratios, surface morphology, grain size, phase structure, and magnetic properties were investigated.

2. Experimental Methods

In order for the substrates to be ready for production, it must be sufficiently clean, and its surface must be smooth. To achieve this, the following steps were followed: 1) the aluminum substrates were

first cleaned in pure water, 2) etched in sodium hydroxide (NaOH) solution, 3) the surface was thoroughly dried and polished, and 4) it was again cleaned with pure water and thoroughly dried.

Experimental Methods

The Co, Ni and CoNi alloys were fabricated as a thin film on an aluminum substrate of 1.7x1.7 cm by electrodeposition method. In order to eliminate the negative effects that can be caused by the substrate in the analysis, thin film coatings were peeled off from the substrate.

In the thin film coating, the electrodeposition process was performed with a three-electrode production system. In this system, a potentiostat was used to provide voltage and current control in the deposition process; a platinum wire was used as a counter electrode; a saturated electrode (SCE) was used as a reference electrode; aluminum substrate was used as the working electrode.

In order to determine the deposition current and potential of each of the Co, Ni, and CoNi alloy thin films, cyclic voltammetry (CV) experiments were carried out at a scanning speed of 10 $mV.s^{-1}$ between +0.5 V and -1.6 V. The pH of the solution was kept constant at 4.5 using sodium hydroxide (NaOH) and hydrochloric acid (HCl) for all the films produced.

In order to achieve a homogeneous distribution, the prepared solutions were stirred 20 minutes prior to the experiment and were continuously stirred at 400 rpm during the experiment. Thin film production was carried out galvanically at 50 mA constant direct current (D.C) and 50 °C at a constant temperature.

In the thin film baths, Merck brand high purity materials were used. Bath compositions were prepared by using cobalt sulfate ($CoSO_4.7H_2O$), nickel sulfate ($NiSO_4.6H_2O$), nickel (II) chloride ($NiCl_2.6H_2O$) and boric acid (H_3BO_3) chemical materials are given in Table 1.

Table 1. Co, Ni, and CoNi alloy thin film bath composition and production data

Thin Films	Electrolyte composition ($Mol.lt^{-1}$)			
	$CoSO_4.7H_2O$	$NiSO_4.6H_2O$	$NiCl_2.6H_2O$	H_3BO_3
Co_{100}	0.07	0	0	0.25
$Co_{70}Ni_{30}$	0.07	0.08	0.18	0.25
$Co_{66}Ni_{34}$	0.07	0.10	0.20	0.25
Ni_{100}	0	0.10	0.20	0.25

The production was performed using 50 mL solutions in four different baths. In the experiments, the amount of boric acid (H_3BO_3) was kept constant at 0.25 $Mol.Lt^{-1}$. As seen in Table 1, Co_{100} and Ni_{100} thin film baths were prepared for %100 pure cobalt and %100 pure nickel production. $Co_{70}Ni_{30}$ alloy thin film bath was prepared from the electrolyte composition Co^{2+} (%24.8) and Ni^{2+} (%75.2). $Co_{66}Ni_{34}$ alloy thin film bath was prepared from the electrolyte composition Co^{2+} (% 22.2) and Ni^{2+} (%77.8). When the $Co_{66}Ni_{34}$ bath content is compared with the $Co_{70}Ni_{30}$ alloy thin film production bath, it is seen that the amount of Co^{2+} metal ions increased (24.8%) and the amount of Ni^{2+} (%75.2) metal ions decreased.

The crystallographic structure of thin films was analyzed using a Rigaku trademark X-ray diffractometer (XRD) device. XRD measurements were performed at 30 mA, 40 kV, between 5° and 90° at a scanning rate of 3.0251 degrees/min. Surface morphological properties of the deposited films were analyzed by Scanning Electron Microscope (SEM, JEOL JSM-5500LV, Japan). In order to determine the amount of Ni and Co concentration in the thin films, Inductive Coupled Plasma (ICP) experiments were performed. The magnetic properties of the thin films were measured with Vibrating

Sample Magnetometer (VSM). VSM measurements were performed at a constant temperature of 300 K and in the range of -75 to +75 kOe. Magnetization (emu/gr) was measured by magnetic field change and the hysteresis curve was obtained using magnetization (emu/gr) values.

3. Results and Discussion

The electrochemical characterization of Co, Ni, and CoNi alloy thin film baths was performed with cyclic voltammetry experiments on aluminum substrates (2.89 cm^2) at a scanning speed of 10 $mV.s^{-1}$. The effects of Ni, Co, and CoNi ions on the hydrogen evolution reaction (HER) in bath composition were studied by cyclic voltammetry (CV). The current-voltage (I-V) graph of the Co_{100} thin film given in Figure 1 was obtained from the bath consisting of 0.07 $Mol.Lt^{-1}$ $CoSO_4.7H_2O$ and 0.25 $Mol.Lt^{-1}$ H_3BO_3. The cyclic voltammetry (CV) experiments were performed between 0.6 V and -1.6 V polarization values. As shown in the graph in Figure 1, no deposition was formed on the substrate until -0.81 V and the anodic current remained constant until this value. However, over this value, it was seen that the discharge started with a rapid increase in the cathodic direction and the deposition started with the bubbles accompanied by the hydrogen gas outlet. When the negative polarization was -1.6 V, it was seen that the current value reached -0.032 A, with the start of the reverse direction scanning, the dissolution was started with the positive current in -0.63 V. Due to the difference between deposition and dissolution potentials, a crossover between anodic and cathodic currents occurs [33]. This crossover indicates the formation of nucleation on the electrode [34].

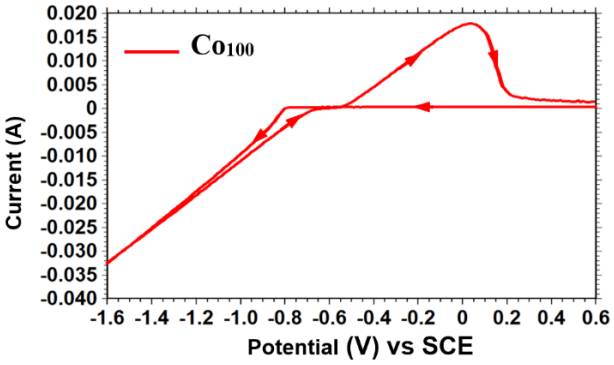

Figure 1. Co_{100} thin film production bath composition; CV experiment (I-V) graph consisting of 0.07 $Mol.L^{-1}$ $CoSO_4.7H_2O$ and 0.25 $Mol.Lt^{-1}$ H_3BO_3 (pH = 4.5, scanning rate = 10 $mV.s^{-1}$)

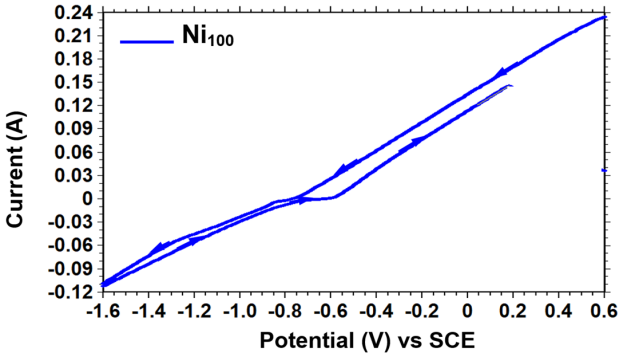

Figure 2. Ni_{100} thin film production bath composition; CV experiment (I-V) graph consisting of 0.10 $Mol.Lt^{-1}$ $NiSO_4.6H_2O$, 0.20 $Mol.Lt^{-1}$ $NiCl_2.6H_2O$ and 0.25 $Mol.Lt^{-1}$ H_3BO_3 (pH = 4.5, scanning rate = 10 $mV.s^{-1}$)

Figure 2 shows the graphic (I-V) of the CV experiment performed in the bath composition for the production of the Ni_{100} thin film. As shown in the graph, when a positive voltage of 0.6 V was applied, the current started to flow in the anodic direction, the deposition began when the applied voltage reached -0.77 V in a negative direction. When the voltage applied in the negative direction, the current at -1.6 V voltage reached the maximum value of -0.109 A. When the voltage was applied to the positive direction from the negative direction, it was seen that the film started to dissolve by flowing in the positive direction at -0.63 V.

The CV experiment (I-V) graphs given in Figure 3 were obtained from the Co_{100}, Ni_{100}, $Co_{70}Ni_{30}$ and $Co_{66}Ni_{34}$ thin film baths in Table 1. When the graphs are examined, the deposited potentials vary between -0.77 and -0.81 V, with the potential applied in the positive direction, the anodic current flow occurs between -0.63 and -0.58 V and the dissolution started in the deposited films. The deposition potential of pure Co^{2+} ions were highest (-0.81 V) compared to the others. In CoNi alloy baths, when the Co^{2+} metal ion content decreased, the dissolution potential decreased (-0.58 V) and the current in

the cathodic direction increased [35]. The indicator of deposition is the hydrogen gas outlet and the accompanying small bubbles. With the increased current in the cathodic direction, hydrogen gas output and accompanying bubbles were observed to increase and CoNi began to deposit on the substrate as a discharge [36]. Depending on the bath composition and the potential value applied, it was seen that the deposition current intensity changed as shown in the graph in Figure 3.

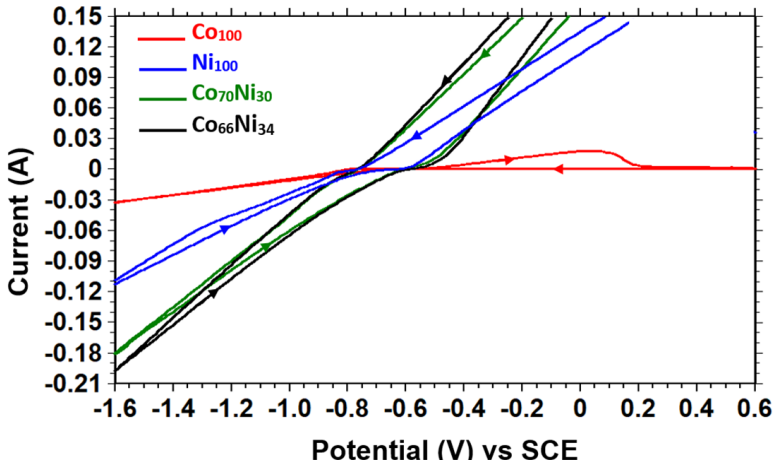

Figure 3. CV experiment (I-V) graphs for the production of Co_{100}, Ni_{100}, $Co_{70}Ni_{30}$ and $Co_{66}Ni_{34}$ thin films

The amount of metal ion concentration in the thin films fabricated was determined by ICP analysis and the results are given in Table 2. Co_{100} thin film was fabricated only from the solution containing Co^{2+} metal ions. In the same way, Ni_{100} thin film was produced only from the solution containing Ni^{2+} metal ions. As shown in Table 2, the amount of Co^{2+} ion in the $Co_{66}Ni_{34}$ film bath was 22.2%, Ni^{2+} metal ion 77.8%, while the Co in the deposited thin film was determined to be 65.6%, Ni 34.4%. Similarly, the amount of Co^{2+} ion in the $Co_{70}Ni_{30}$ film bath was 24.8% and Ni^{2+} metal ion 75.2%; while the Co in the deposited thin film was determined to be 70.37% and Ni 29.63%. As can be seen from the values given in Table 2, the percentage ratios of Co^{2+} and Ni^{2+} ions in the electrolyte bath composition and the percentage ratios of Co-Ni materials in the deposited $Co_{70}Ni_{30}$ and $Co_{66}Ni_{34}$ films are different from each other. We think that this difference in the deposition of CoNi alloys is due to the anomalous deposition behavior of Co and Ni during deposition. The anomalous deposition is the preferential deposition of cobalt Co^{2+} metal ions, which are less noble than Ni^{2+} metal ions, on the cathode surface [37-38]. The functional properties of the electrodeposited NiCo alloys are strongly dependent on their bath composition and deposition parameters. To understand the cause of anomalous deposition, it is important to understand the effects of deposition parameters on bath composition and deposition. It has been reported in the literature that anomalous deposition occurs in the electrodeposition of iron metals (cobalt, nickel and iron) and zinc with iron metals [39-42].

In anomalous deposition, it is reported that higher Co content is always deposited on the film compared to the ratio of Co^{2+} metal ions and Ni^{2+} metal ions in the bath content. In the co-deposition of Ni-Co as an alloy film, the electrodeposition of Co is controlled by diffusion, while the electrodeposition of Ni is controlled by activation. Increasing the cathodic current density causes an increase in the cathodic overpotential, accompanied by increased activation of the electrode reaction. The cathodic current, which increases in the negative direction under the overpotential, causes an increase in the Ni content deposited in the film. Thus, an increase in current density causes a decrease in the Co content of the deposited material [43].

As seen in the values given in Table 2, when the amount of Co in the Co-Ni bath decreases from 24.8% to 22.2%, the amount of Ni increases from 75.2% to 77.8%. Meanwhile, the cathodic current

value passing in the negative direction increases from 0.180 A to 0.198 A, as seen in the CV graph in Figure 3, and it is seen that the amount of Ni deposited in the film increases (Table 2) [39,44].

Table 2. Co and Ni matter amount ratios in thin film and electrolyte contents

Thin Films	Electrolyte Composition		Film Composition	
	% Co	%Ni	% Co	%Ni
Co_{100}	100	0	100	0
$Co_{70}Ni_{30}$	24.80	75.20	70.37	29.63
$Co_{66}Ni_{34}$	22.20	77.80	65.60	34.40
Ni_{100}	0	100	0	100

By varying the concentration of Co^{2+} and Ni^{2+} metal ion in the electrolyte, it is possible to fabricate CoNi alloys of a wide range of compounds by electrodeposition. The components forming the alloys compared to the single metal type may exhibit more interesting structural, electronic, and magnetic properties due to their interaction with each other [5]. The magnetic properties of CoNi alloy thin films can show hard magnetic and soft magnetic material behavior depending on the Co and Ni concentration ratio. Therefore, Ms, Hc and Mr values may vary according to film content [45].

The crystal structures of the electrodeposited thin films were analyzed by XRD experiments and the measurement results were given on graphs in Figure 4. In the analysis, Co_{100}, Ni_{100}, $Co_{70}Ni_{30}$, $Co_{66}Ni_{34}$ films were found to have a crystal structure, Ni_{100} film XRD peaks were strong and others were weaker ($Co_{70}Ni_{30}$, $Co_{66}Ni_{34}$ and Co_{100}). The crystal structure of the Ni_{100} thin film was determined on the surface centered cubic (FCC) and β phase preferentially orientation (111) (200) and (220) plane. XRD analyses were determined by comparison with ICDD (01-070-0989) data [46]. The lattice constant of the Ni_{100} thin film obtained from the XRD data was found to be a = 3.518764 Å. Co_{100} thin film was found in the volume-centered cubic (HCP) structure, in the α phase and in the most dominant peak orientation (002) plane. The lattice constants a (A) = 2.506107 Å, b (A) = 2.506107 Å, c (A) 4.068314 Å were found to be compared to the data of (ICDD, 01-071-4239) [47-49].

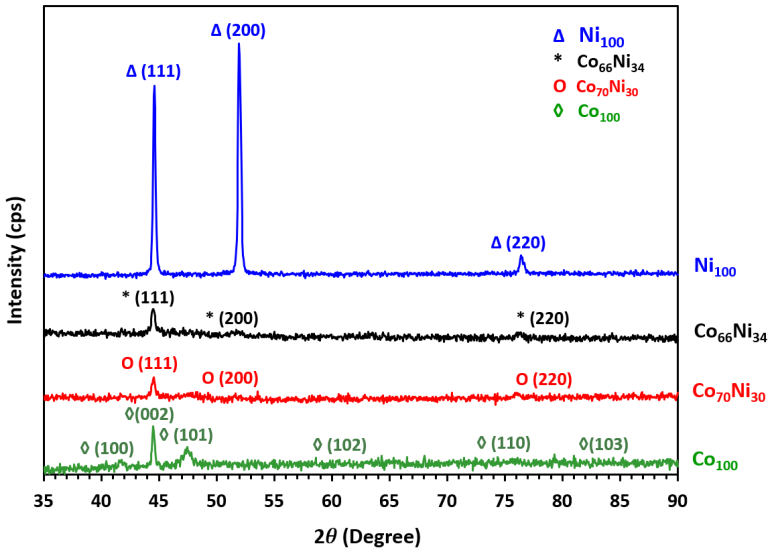

Figure 4. Graph of XRD analysis results of thin films (Co_{100}, $Co_{70}Ni_{30}$, $Co_{66}Ni_{34}$, Ni_{100})

Considering CoNi binary alloy phase diagrams, it is reported that when the Ni content is less than 25%, the phase structure is HCP and when it is greater than 25%, the structure is FCC [50]. As can be seen from the ICP results given in Table 2, it was found that the amount of Ni in CoNi alloys was

greater than 25%. In Figure 4, XRD graphs of $Co_{70}Ni_{30}$ and $Co_{66}Ni_{34}$ alloy films were given. The crystal orientation of the alloys was determined to be dominant peaks (111), the FCC structure, β phase (ICDD, 01-074-5694) and the results were consistent with the literature [51-52].

Table 3. Co, Ni and CoNi alloys XRD analysis results

Thin Films	2-Θ (deg.)	d Å (ang.)	Intensity (cps)	FWHM	Lattice (Å)			Grainsize (nm)
					a	b	c	
Co_{100}	44.50	2.0342	392	0.210	2.506107	2.506107	4.068314	42.3
$Co_{70}Ni_{30}$	44.48	2.0350	192	0.330	3.524968	3.524968	3.524968	27.3
$Co_{66}Ni_{34}$	44.50	2.0345	238	0.310	3.523863	3.523863	3.523863	29.2
Ni_{100}	51.95	1.7586	2676	0.213	3.518764	3.518764	3.518764	43.3

The grain size of the CoNi alloys was calculated with the Debye-Scherer formula given in equation 1. The grain size was found using the FWHM value of the greatest intensity of the peak given in Table 3 [53].

$$D = \frac{0.9\lambda}{\beta \cos\theta} \tag{1}$$

where D is the grain size, β FWHM value, λ X-ray wavelength and θ value is the X-ray diffraction angle. The analysis results in Table 3 showed that the grain sizes of Co and Ni films were 42.3 nm and 43.3 nm respectively, but the grain sizes decreased when they formed the binary metal alloy ($Co_{70}Ni_{30}$, $Co_{66}Ni_{34}$) (27.3 nm, 29.2 nm). The reason is why Co and Ni substances have better properties than a single metal when formed a binary alloy [5]. The amount of cobalt-nickel material in the CoNi alloy, the deposited current and the additives affect the grain size and the grain size is particularly effective on Hc [54-55]. Figure 5 shows SEM images taken to examine the morphological characteristics of thin films produced. The morphological characteristics of the film surfaces differed according to the amount of material and the grain size of the film content, crystallization occurred and was consistent with the XRD results.

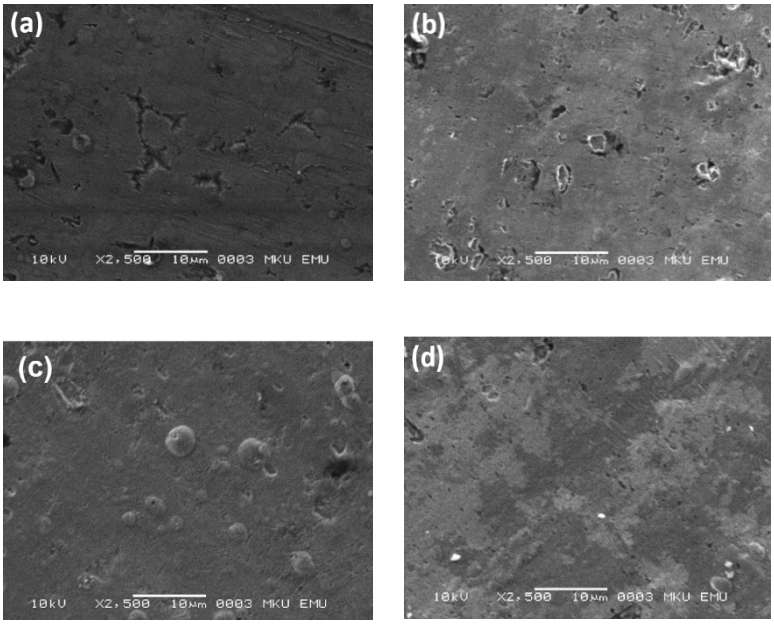

Figure 5. SEM images of Co, Ni and CoNi thin films; (a) Co_{100}, (b) $Co_{70}Ni_{30}$ alloy, (c) $Co_{66}Ni_{34}$ alloy, (d) Ni_{100}

To examine the magnetic properties, VSM analysis measurements were performed at a constant room temperature of 300 K. The magnetization (emu/gr) values of the fabricated Co_{100}, Ni_{100}, $Co_{70}Ni_{30}$, $Co_{66}Ni_{34}$ films were measured by changing the magnetic field strength between -75000 Oe to 75000 Oe, and the hysteresis loops given in Figure 6 and Figure 7 were obtained. The Ms was found in the hysteresis loops given in Figure 6 Hc which are the inverse force in the opposite direction and Mr values were found from the curves given in Figure 8 and the results were given in Table 4. The magnetic measurement results showed that Co, Ni, and CoNi alloy thin films exhibited ferromagnetic behavior and were hard magnetic materials [56].

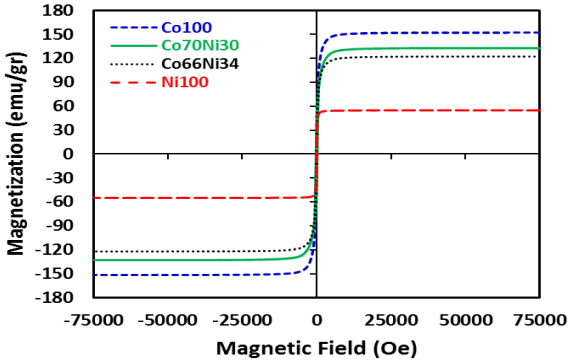

Figure 6. Magnetization curves measured against magnetic field applied to thin films between +75000 and -75000 Oe

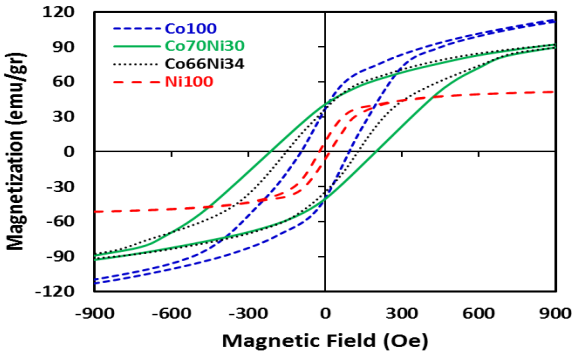

Figure 7. Magnetization curves (hysteresis loops) measured against magnetic field applied between +900 and -900 Oe

Table 4. Hysteresis loops analysis results

Thin Films	Hc (Oe)	Mr (emu/gr)	Ms (emu/gr)
Co_{100}	93.0	38.80	152.276
$Co_{70}Ni_{30}$	206.0	41.08	132.541
$Co_{66}Ni_{34}$	139.0	35.46	122.287
Ni_{100}	13.8	5.17	55.027

The magnetization of any material is related to the number of magnetic moments it has under an external magnetic field. The number of magnetic moments per unit volume gives the magnitude of magnetization. When the magnetic field value is increased in the (+) or (-) direction in ferromagnetic materials, the magnetic moments are aligned in the magnetic field direction and after a certain value, the magnetization value is not changed. This value is called Ms [29,57]. In the literature, the saturation magnetization values of pure Co and Ni materials are given as 0.48 10^6 $A.m^{-1}$ for Ni and 1.40 10^6 $A.m^{-1}$ for Co (at 300 K). Co has a larger magnetic dipole moment than a Ni [29]. In Figure 6, the value of Ms that occurred on thin films was measured at 55.02 emu/gr on the lowest Ni_{100} film of the highest Co_{100} (152.27 emu/gr) against the change of the applied magnetic field strength. When CoNi formed a binary alloy, the Co content in the film was 70.37% while the Ms value was 132.54 emu/gr and when the Co content was 65.60% the value of Ms was measured as 122.28 emu/gr. Increasing the amount of Co in the CoNi alloy film content causes an increase in the total magnetic moment. Accordingly, the Ms value increases with the increase in the amount of Co. Likewise, it can be said that the Ms value decreases with the increase of the Ni amount [28]. These results show that the Ms value on the films increases or decreases proportionally with the amount of Co [58-59].

When the external magnetic field effect is zero, the magnetization value remaining on the material is called Mr (remanence or residual magnetization). Permanent magnetization; It changes with

polarization, which occurs depending on the pole force of magnetization acting on the material, and the shape of the material [29]. Mr values were found from the hysteresis loops given in Figure 8 and given in Table 4. When CoNi formed a binary alloy, Ms was better than Co_{100} (38.80 emu/gr) and Ni_{100} (5.17 emu/gr). These results showed that as the amount of Co decreased, the value of Mr decreased [60-61].

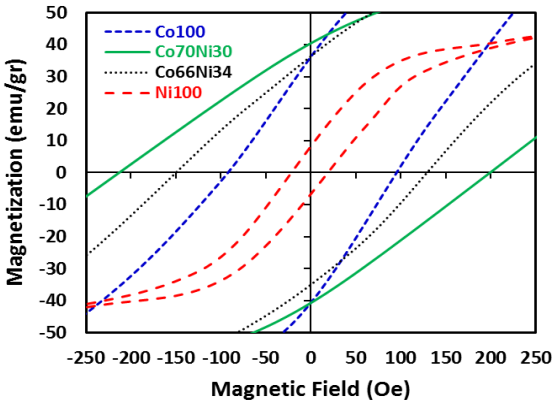

Figure 8. Magnetization curves (hysteresis loops) measured against magnetic field applied between +250 and -250 Oe

The Hc is the magnetic field strength applied to zero the Mr value on the material in the opposite direction. The Hc values of magnetic materials are greatly influenced by grain size and magneto crystal anisotropy. The reduction of the grain size in the magnetic material results in a decrease in the magnitude of the magnetic field force that has to be applied, which leads to a decrease in Hc values. Materials with a Hc value less than 12.6 Oe are called soft magnetic materials, and materials with a Hc value greater than 12.6 Oe are called hard magnetic materials [29, 50]. In the graph in Figure 9, the grain size and the change of Hc value were given graphically depending on the amount of Co in the CoNi alloy film. In the graph in Figure 9, the grain size and Hc value change were given graphically depending on the amount of Co in CoNi alloy film. As shown in the graph, the Hc value of Co_{100} was found to be 93 Oe and Ni_{100} 13.8 Oe, but when CoNi binary alloy ($Co_{70}Ni_{30}$, $Co_{66}Ni_{34}$) formed, the Hc value increased to 206 Oe. The major change in the Hc value can be explained by the change in the crystal and phase structures of thin films. In the XRD analysis, for the Co_{100}, it was found the structure was in the HCP and the phase was α phase, for the Ni, it was found the structure was in the FCC and the phase was β phase. and in the FCC structure and β phase when the CoNi binary alloy was formed. This change in crystal and phase structures leads to a great change in the grain size and magneto crystal anisotropy [62].

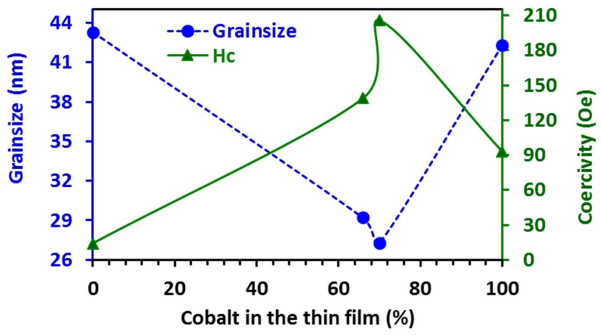

Figure 9. The change in grainsize and Hc according to the amount of Co in the film content

The Hc values of all the thin films fabricated showed that they were hard magnetic materials. In these materials, the Hc of the Ni_{100} thin film showed property close to the soft material (13.8 Oe). The change in CoNi alloy Hc value depends on the amount of Co in the film. Since Co^{2+} ions in the film

have larger magneto-crystal anisotropy and magnetic moment than Ni^{2+} ions, the Hc value increases when the Co amount increases [62-63]. The amount of Co in the content of alloy thin film and the grain size varies depending on the composition of the bath, deposition current, pH, temperature, and additives. By controlling these variables in the bath composition, it is possible to produce smaller grain size CoNi alloy materials [64]. Thus, the desired materials with hard magnetic and soft magnetic material properties can be fabricated.

This study indicated that the properties of the thin films can be controlled by the electrodeposition parameters. The results of the analysis of the Co, Ni, and CoNi alloy thin films fabricated are compatible with the literature and we believe that they will contribute to future studies.

4. Conclusions

Co, Ni, and CoNi alloy thin films were fabricated by electrodeposition method and their structural and magnetic properties were investigated.

The catalytic properties of the CoNi alloy thin films bath composition were better than Co_{100} and Ni_{100} thin films and the deposition overpotential was lower. As seen in the CV experiments, the change in the I-V value affects the hydrogen evolution reaction and the energy consumed during deposition.

As a result of XRD analysis, the crystal structure of Co was found in the HCP and α phase, Ni was in FCC structure and β phase, and CoNi alloys were in FCC structure and β phase. The grain size was largely influenced by crystal phase structure and the ratio of Co-Ni matter in the thin film content, and varied between 27.3 nm and 43.3 nm, and the grain size was smaller in alloys compared to Co and Ni single metals.

For the determination of magnetic properties, VSM analysis was performed and the magnetic moment (emu/gr) values were measured in the face of the magnetic field strength between -75000 Oe, and +75000 Oe and hysteresis loops were obtained.
The Hc values of Co_{100}, Ni_{100} , and CoNi alloy thin films were found between 13.8 - 206 Oe, Ms ranged between 55.02-152.27 emu/gr and Mr ranged from 5.17-41.08 emu/gr. All of the thin films fabricated have been confirmed by the hysteresis loops, where they exhibit the behavior of hard magnetic and ferromagnetic materials.

It was seen that Co and Ni concentration ratio, grain size and magneto crystal anisotropy in the alloy film can be controlled by the bath composition and the desired hard magnetic and soft magnetic materials can be fabricated.

Acknowledgments

Financial support for this research by the Kilis 7 Aralık University Scientific Research Projects is gratefully acknowledged (BAP-2014/02/LTP/05).

Authors' Contributions

RÖ and CAK designed the structure. CAK grew the sample according to the specifications. CAK carried out the experiments work, the theoretical calculations, in collaboration with RO. RO wrote up the article. RÖ is the coordinator of the project and the supervisor of CAK.

Both authors read and approved the final manuscript.

Competing Interests

The authors declare that they have no competing interests.

Refereneces

[1]. Marikkannu K.R., Paruthimal Kalaignan G., Vasudevan T., "The role of additives in the electrodeposition of nickel–cobalt alloy from acetate electrolyte", Journal of Alloys and Compounds, 2007, 438: 332-336.

[2]. Sharma A., Chhangani S., Madhavan R., Suwas S., "Correlation between crystallographic texture, microstructure and magnetic properties of pulse electrodeposited nanocrystalline Nickel–Cobalt alloys", Journal of Magnetism and Magnetic Materials, 2017, 434: 68-77.

[3]. Arenas J.V., Pritzker M., "Steady-state model for anomalous Co–Ni electrodeposition in sulfate solutions", Electrochimica Acta, 2012, 66: 139-150.

[4]. Özdemir R., "Effect of the Applied Current Density on the Structural and Magnetic Properties of the Electrodeposited Cobalt-Nickel Alloy Thin Films", Acta Physica Polonica A, 2017, 132 (3): 770-774.

[5]. Xu C., Nie D., Chen H., Wang Y., Liu Y., "Template-free synthesis of magnetic CoNi nanoparticles via a solvo thermal method", Materials Letters, 2015, 138: 158 -161.

[6]. Bekish YN., Poznyak SK., Tsybulskaya LS., Gaevskaya TV., Kukareko VA., Mazanikc AV., "Electrodeposited Ni-Co-B Alloy Coatings: Preparation and Properties", Journal of The Electrochemical Society, 2014, 161 (12): D620-D627.

[7]. Fukui R., Katayama Y., Miura T. The effect of organic additives in electrodeposition of Co from an amide-type, ionic liquid. Electrochimica Acta. 2011, 56: 1190-1196.

[8]. Lupi C., Dell'Era A., Pasquali M. Effectiveness of sodium citrate on electrodeposition process of Ni-Co-W alloys for hydrogen evolution reaction. Int J Hydrogen Energy. 2017, 42: 28766-28776.

[9]. Özdemir R., Karahan İ.H., Karabulut O., "A Study on the Electrodeposited Cu-Zn Alloy Thin Films", Metallurgical and Materials Transactions A, 2016, 47 (11): 5609-5617.

[10]. Karahan İ.H., Ozdemir R., "Genetic programming modelling for the electrical resistivity of Cu–Zn thin films", Pramana - J Phys 2018, 91:42.

[11]. Xu Q., Sun CX., Wang ZJ., Liu JJ., Ren YX., Hao SZ., Zhu JL., Sun YB., Sun HY., "Preparation and characterization of iridescent $Ni_{1-x}Co_x$ containing anodic aluminum oxide films", Dyes and Pigments, 2017, 147: 313-317.

[12]. Zhou C., Du H., Li H., Qian W., Liu T., "Electrode based on nanoporous (Co-Ni)@(CoO, NiO) nanocomposites with ultrahigh capacitance after activation", Journal of Alloys and Compounds, 2019, 778: 239-246.

[13]. Lee C.K., "Effects of hydrogen and oxygen on the electrochemical corrosion and wear-corrosion behavior of diamond films deposited by hot filament chemical vapor deposition", Applied Surface Science, 2008, 254: 4111-4117.

[14]. Noor A., Azura M.A., Chin S.F., "Impact on Development of ZnS Nanoparticles Thin Film Deposited by Chemical Bath Deposition and Spin Coating", International Journal of Advanced Engineering and Nano Technology (IJAENT) 2021, 4:5.

[15]. Özdemir R., Karahan İ.H., "Electrodeposition and properties of Zn, Cu, and Cu1−xZnx thin films", Applied Surface Science, 2014, 318: 314–318.

[16]. Lee K., Kang J., Jin S., Lee S., Bae J., "A novel sol-gel coating method for fabricating dense layers on porous surfaces particularly for metal-supported SOFC electrolyte", Int J Hydrogen Energy, 2017, 42: 6220-6230.

[17]. Zaremba O.T., Goldt A.E., Khabushev E.M., Anisimov A.S., Nasibulin A.G., "Highly efficient doping of carbon nanotube films with chloroauric acid by dip-coating", Materials Science and Engineering B, 2022, 278:115648.

[18]. Maosen Z., Shujiang G., Gang C., Fuhui W., Douglas G.I., "Sputtered Fe1·5CoNi0.5 coating: An improved protective coating for SOFC interconnect applications", International Journal of Hydrogen Energy, 2022, 47:22, 11658-11668.
[19]. Sarigül H., Özçeşmeci M., Sorar İ., "Sol-Jel Yöntemiyle Hazırlanan Kobalt Ftalosiyanin Katkılı TiO2 Filmlerin Optik ve Yapısal Özelliklerinin İncelenmesi", El-Cezerî Journal of Science and Engineering, 2021, 8:1, 299-308.
[20]. Yang Q., Lv C., Huang Z., Zhang C., "Amorphous film of ternary Ni-Co-P alloy on Ni foam for efficient hydrogen evolution by electroless deposition", Int J Hydrogen Energy, 2018, 43: 7872-7880.
[21]. Zhu Y.L., Katayama Y., Miura T., "Effects of coumarin and saccharin on electrodepositionof Ni from a hydrophobic ionic liquid", Electrochimica Acta, 2014, 123: 303-308.
[22]. Sahin B., Bayansal F., Yuksel M., Biyikli N., Çetinkara HA., "Effect of coumarin concentration on the physical properties of CdO nanostructures. Ceramics International", 2014, 40: 5237-5243.
[23]. Özdemir R., Korkmaz C.A., Karahan İ.H., "Investigation of the structural and magnetic properties of the cobalt-nickel alloys fabricated in various electrolyte solutions", Acta Physica Polonica A, 2017, 132:3, 1045-1049.
[24]. Liu F., Deng Y., Han X., Hu W., Zhong C., "Electrodeposition of metals and alloys from ionic liquids. Journal of Alloys and Compounds", 2016, 654: 163-170.
[25]. Brenner A., "Electrodeposition of Alloys Principles and Prattice", Chap. Academic Pres. NewYork, 1963: 457.
[26]. Aktas S., Yavuz A., Kaplan K., Bedir M., "Electrochemical Behavior of Tin Based Film Cathodically Deposited from Non-Aqueous Media", Cezerî Journal of Science and Engineering", 2020, 7:2, 639-648.
[27]. Fenineche N., Coddet C., "Effect of Electrodeposition Parameters On The Microstructure And Mechanical Properties Of Co-Ni Alloys", Surface and Coatings Technology, 1990, 41: 75-81.
[28]. Karpuz A., Kockar H., Alper M., "Effect of film thickness on properties of electrodeposited Ni–Co films", Applied Surface Science, 2012, 258: 5046–5051.
[29]. Jiles D., "Introduction to Magnetism and Magnetic Materials", Department of Materials Science and Engineering, Iowa State University, USA, ISBN 978-1-4615-3868-4 (eBook), 1991:440.
[30]. Esteves M.C., Sumodjo P.T.A., Podlaha E.J., "Electrodeposition of CoNiMo thin films using glycine as additive: anomalous and induced code position", Electrochimica Acta, 2011, 56: 9082– 9087.
[31]. Das A., "Prodding Magnetic Properties of Electrodeposited Co/Cu and Ni/Cu alloy Films by Scanning Probes", Master Thesis, Department of Metallurgical and Materials Engineering. National Institute of Technology, 2010.
[32]. Ergeneman O., Sivaraman K.M., Pané S., Pellicer E., Teleki A., Hirt A.M., Baró M.D., Nelson B.J., "Morphology, structure and magnetic properties of cobalt–nickel films obtained from acidic electrolytes containing glycine", Electrochimica Acta, 2011, 56: 1399–1408.
[33]. Kemp T.J., "Instrumental Methods in Electrochemistry", Southampton Electrochemistry Group, in: T.J. Kemp (Ed.), Ellis Horwood Ltd. Chichester, UK. 1985.
[34]. Grujicic D., Pesic B., "Electrodeposition of copper, the nucleation mechanisms". Electrochimica Acta", 2002, 47: 2901-2912.
[35]. G´omez E., Pan´e S., Alcobe X., Vall´es E., "Influence of a cationic surfactant in the properties of cobalt–nickel electrodeposits", Electrochimica Acta, 2006, 51: 5703–5709.
[36]. Darband G.B., Aliofkhazraei M., Rouhaghdam A.S., Kiani M.A., "Three-dimensional Ni-Co alloy hierarchical nanostructure as efficient nonnoble- metal electrocatalyst for hydrogen evolution reaction" Applied Surface Science, 2019, 465: 846–862.
[37]. Karpuz A., Kockar H., Alper M., Karaagac O., Haciismailoglu M., "Electrodeposited Ni–Co films from electrolytes with different Co contents", Applied Surface Science, 2012, 258: 4005-4010.

[38]. Olvera S., Estrada E.M.A., Marcos J.S., Palomares F.J., Vazquez L., Herrasti P., "Effect of the low magnetic field on the electrodeposition of Co_xNi_{100-x} alloys", Materials Characterization, 2015, 105: 136-43.
[39]. Sknar Yu.E., Sknar I.V., Savchuk O.O., Danilov F.I., "Electrodeposition of Ni-Co alloy from methansulfonate electrolyte. The role of the electrolyte pH in the anomalous codeposition of nickel and cobalt", Surface & Coatings Technology, 2020, 387: 125542.
[40]. Fan C., Piron D.L., "Study of anomalous nickel-cobalt electrodeposition with different electrolytes and current densities", Electrochmica Acta., 1996, 41(10), 1713-1719.
[41]. Vazquez-Arenasa J., Altamirano-Garciab L., Treeratanaphitaka T., Pritzkera M., Sánchezb R.L., Sierrac R.C., "Co–Ni alloy electrodeposition under different conditions of pH, current and Composition", Electrochimica Acta, 2012, 65: 234-243.
[42]. Tian L., Xu J., Xiao S., "The influence of pH and bath composition on the properties of Ni-Co coatings synthesized by electrodeposition", Vacuum, 2011, 86: 27.
[43]. Li Y., Jiang H., Huang W., Tian H., "Effects of peak current density on the mechanical properties of nanocrystalline Ni–Co alloys produced by pulse electrodeposition", Applied Surface Science, 2008, 254: 6865-6869.
[44]. Barati Darband Gh., Aliofkhazraei M., Sabour Rouhaghdama A., Kianib M.A., "Three-dimensional Ni-Co alloy hierarchical nanostructure as efficient non noble- metal electrocatalyst for hydrogen evolution reaction", Applied Surface Science, 2019, 465: 846-862.
[45]. Moskaltsova A., Proenca M.P., Nedukh S.V., Sousa C.T., Vakula A., Kakazei G.N., Tarapov S.I., Araujo J.P., "Study of magnetoelastic and magneto crystalline anisotropies in CoxNi1-x nanowire arrays", Journal of Magnetism and Magnetic Materials, 2015,374: 663-668.
[46]. Rafique M.Y., Pan L., Farid A., "From nano-dendrite to nano-sphere of Co100-xNix alloy: Composition dependent morphology, structure and magnetic properties", Journal of Alloys and Compounds, 2016, 656: 443-451.
[47]. Rafailović L.D., Minić D.M., "Deposition and Characterisation of Nanostructured", Hem. ind. 2009, 63 (5a): 557-569.
[48]. Tian H., Khanaki A., Das P., Zheng R., Cui Z., He Y., Shi W., Xu Z., Lake R., Liu J., "Role of Carbon Interstitials in Transition Metal Substrates on Controllable Synthesis of High-Quality Large-Area Two-Dimensional Hexagonal Boron Nitride Layers", Nano Letters, 2018, 18 (6): 3352-3361.
[49]. Armyanov S., "Crystallographic structure and magnetic properties of electrodeposited cobalt and cobalt alloys", Electrochimica Acta, 2000, 45: 3323-3335.
[50]. Samardak S., Nasirpouri F., Nadi M., Sukovatitsina EV., Ognev AV., Chebotkevich LA., Komogortsev S.V., "Electrodeposition of nanostructured CoNi thin films and their anomalous infrared properties", J. Magnetism Magnetic Mater, 2015, 383: 94-99.
[51]. Teber A., Unver I., Kavas H., Aktas B., Bansal R., "Knitted radar absorbing materials (RAM) based on nickel–cobalt, magnetic materials", Journal of Magnetism and Magnetic Materials, 2016, 406: 228-232.
[52]. Elrouby M., El-Lateef H.M.A., Sadek M., "Electrodeposited Pt nanorods on a novel flowered-like nanostructured Ni-Co alloy as an electrocatalyst for methanol oxidation", Int J Hydrogen Energy, 2019, 44: 13820-13834.
[53]. Djamal M., Ramli, Khairurrijal and Haryanto F., "Development of Giant Magnetoresistance Material Based on Cobalt Ferrite", Acta Physica Polonica, 2015, 128: No. 2-B; 19-22.
[54]. Madhavan R., Suwas S., "Evolution of deformation texture and magnetic properties in a nanocrystalline nickel-20 wt% cobalt alloy", Journal of Magnetism and Magnetic Materials, 2015, 378: 239-245.
[55]. Noori F., Ramazani A., Kashi M.A., "Controlling structural and magnetic properties in CoNi and CoNiFe nanowire arrays by fine-tuning of Fe content", Journal of Alloys and Compounds. 2018, 756: 193-201.
[56]. Laslouni W., Azzaz M., "Electromagnetic Properties in Nanostructured Alloy Cu70Co30 Obtained by a Non-Equilibrium Method", Acta Phys. Pol. A, 2016, 130: 112-114.

[57]. Michael E. Mchenry, David E. Laughlin, “Magnetic Moment and Magnetization”, Carnegie Mellon University, 2012, John Wiley & Sons, Inc., edited by Elton N. Kaufmann, Pittsburgh, PA, USA.
[58]. Karpuz A., Kockar H., Alper M., “The effect of different chemical compositions caused by the variation of deposition potential on properties of Ni–Co films”, Applied Surface Science, 2011, 257: 3632-3635.
[59]. Cojocaru P., Magagnin L., Gómez E., Vallés E., “Electrodeposition of CoNi and CoNiP alloys in sulphamate electrolytes”, Journal of Alloys and Compounds, 2010, 503: 454-459.
[60]. Chen Q.S., Zhou Z.Y., Guo G.C., Sun S.G., “Electrodeposition of nanostructured CoNi thin films and their anomalous infrared properties”, Electrochimica Acta, 2013, 113: 694-705.
[61]. Ho C.Y., Lin T.H., Chang Y.J., “Influence of various annealed Ni-Co nanowire properties upon the capability of immobilization of histidine-tagged protein”, Journal of Alloys and Compounds, 2015, 648: 726-731.
[62]. Xu J., Xu Y., “Fabrication and magnetic property of binary Co–Ni nanowire array by alternating current electrodeposition”, Applied Surface Science, 2007, 253: 7203-7206.
[63]. Xu Q., Wang Z.J., Wang Y.G., Sun H.Y., “The effect of Co content on the structure and the magnetic properties of Co_xNi_{1-x} nanotubes”, Journal of Magnetism and Magnetic Materials, 2016, 419: 166-170.
[64]. Ciszewski A., Posluszny S., Milczarek G., Baraniak M., “Effects of saccharin and quaternary ammonium chlorides on the electrodeposition of nickel from a Watts-type electrolyte”, Surface and Coatings Technology, 2004, 183: 127–133.